JOURNAL OF CATALYSIS 157, 403–413 (1995)

Mechanisms of Methanol Synthesis from Carbon Dioxide and from Carbon Monoxide at Atmospheric Pressure over Cu/ZnO

Shin-ichiro Fujita, Masahito Usui, Hiroto Ito, and Nobutsune Takezawa

Division of Materials Science and Engineering, Faculty of Engineering, Hokkaido University, Sapporo, 060, Japan

Received January 26, 1995; revised July 31, 1995; accepted August 2, 1995

Methanol synthesis from CO_2 and CO was carried out at atmospheric pressure over a Cu/ZnO catalyst (Cu/Zn = 3/7) and the surface species formed were analyzed by diffuse reflectance FT-IR spectroscopy and temperature programmed desorption. It was revealed that CH_3OH and CO were produced from CO_2–H_2 through parallel pathways. Two types of formate species, HCOO–Cu and HCOO–Cu and HCOO–Zn, and zinc methoxide were formed in the course of methanol synthesis from CO_2. HCOO–Cu and HCOO–Zn were hydrogenated to methoxide. A comparison of the rates of hydrogenation with that of methanol synthesis from CO_2 suggested that methanol synthesis from CO_2 occurred via the hydrogenation of HCOO–Cu. The methanol synthesis from CO proceeded at a rate much slower than that from CO_2. HCOO–Zn and zinc methoxide were formed in the course of the CO–H_2 reaction. No HCOO–Cu was detected. The amount of the zinc methoxide formed in the CO–H_2 reaction greatly exceeded that formed in the CO_2–H_2 reaction. The rate of the formation of methoxide in the CO–H_2 reaction was in reasonable agreement with that of the hydrogenation of HCOO–Zn. On the basis of these findings, the difference in the mechanisms of methanol synthesis from CO_2 and from CO was discussed. © 1995 Academic Press, Inc.

INTRODUCTION

In industrial processes, methanol is synthesized from mixtures of CO, CO_2, and H_2 over Cu/ZnO based catalysts. CO_2 promotes methanol synthesis from CO (1–4). Because of practical and fundamental interests in this promoting effect, methanol synthesis from CO_2 and H_2 has received considerable attention in recent years (5–16). Comparative studies showed that methanol synthesis from CO_2 began at a temperature lower than that from CO and proceeded at a faster rate (6, 7, 13).

By the use of the temperature programmed desorption (TPD), IR spectroscopy, and chemical trapping methods, various surface species such as formate (8, 10, 12, 17–24), formaldehyde (17), dioxymethylene (25), and methoxide species (19–21, 25) were found to exist on Cu based catalysts in the course of methanol synthesis from CO_2. Saussey and Lavalley (19) measured the surface species formed on Cu/$ZnAl_2O_4$ by IR spectroscopy. They showed that an appreciable amount of methoxide was formed on the support in the course of methanol synthesis from CO. Formate species formed on Cu were absent in the course of the CO–H_2 reaction, while these species were present in the course of the CO_2–H_2 reaction. They proposed that methanol synthesis from CO_2 occurred on the Cu surface, while that from CO occurred on the surface of the support. Robinson and Mol (23) suggested that the formate species formed on Cu exhibited different reactivity from that on the support, resulting in the difference in the rates of methanol synthesis from CO_2 and from CO.

In previous work (26, 27), we showed that methoxide on ZnO was readily hydrolyzed to methanol over Cu/ZnO and ZnO in the course of methanol synthesis from CO_2. The presence of H_2O may be a key reason for the difference in the rates of methanol synthesis from CO_2 and from CO, as Saussey and Lavalley proposed (19), since no H_2O was formed in the methanol synthesis from CO–H_2. In these circumstances, the origin of the difference in the rates is still controversial.

In the present work, the methanol synthesis from CO_2 and from CO were carried out over various Cu/ZnO catalysts at atmospheric pressure, and the reactivity of adsorbed species formed over the catalysts was studied by means of diffuse reflectance FT-IR spectroscopy and temperature programmed desorption. We show that methanol synthesis from CO_2 proceeded via the hydrogenation of formate species formed on copper, while that from CO proceeded via the hydrogenation of formate species formed on ZnO. The difference in rate between methanol synthesis from CO_2 and from CO is discussed.

EXPERIMENTAL

Catalyst Preparation

Cu/ZnO catalysts (Cu content = 10, 30, 50, 70, 90 mol%) were prepared by two coprecipitation methods. The catalysts with copper content below 30 mol% were prepared

0021-9517/95 $12.00

TABLE 1

Copper Dispersion, BET Area, and Surface Area of Copper and ZnO of the Cu/ZnO, Cu, and ZnO Catalysts

Cu/Zn	D_{Cu} [%]	S_{BET}[a]	S_{Cu}[a]	S_{ZnO}[a]
10/90	10.4	29.0	4.5	24.5
30/70	9.8	27.9	13.6	14.3
50/50	11.7	41.2	25.8	15.4
70/30	9.6	32.4	29.6	2.8
90/10	5.0	10.6	20.0	—
100/0	1.1	—	4.7	—
0/100	—	39.8	—	39.8

[a] In a unit of m^2/g-cat.

by a coprecipitation method (method 1) similar to that adopted by Herman *et al.* (28). An aqueous solution of Na_2CO_3 (1.5 *M*) was added dropwise to a mixed solution of copper and zinc nitrates (total metal concentration 1 *M*) at 353 K until the pH reached 8.0 and then the solution was aged at 353 K for 1 h. During the aging, the pH was adjusted to 8.0–8.2 by addition of a small amount of Na_2CO_3 solution. The catalysts having copper content above 50 mol% were prepared from copper and zinc nitrates and $NaHCO_3$ by an inverse coprecipitation method (method 2) similar to that adopted by Porta *et al.* (29). A 1 *M* solution of copper and zinc nitrates (50 cm^3) was added dropwise to a 1.2 *M* solution of $NaHCO_3$ (100 cm^3; pH 8.2) over a period of 90 min at 338 K under continuous stirring. The precipitates formed were further aged for 90 min at the same temperature. The precipitates were filtered out, washed with distilled water, dried at 373 K overnight, and calcined in air at 623 K for 4 h. The catalyst thus prepared was first reduced in a reactor or in an IR cell under a helium stream containing 3 vol% of H_2 at 483 K for 1 h. The reduction temperature was raised from 483 to 523 K stepwise by 10 K per hour and finally kept at 523 K for 1 h under a pure H_2 stream.

ZnO and pure copper catalysts were obtained by precipitation in similar fashions to methods 1 and 2, respectively. Procedures following the precipitation were the same as those for the Cu/ZnO catalysts.

Table 1 lists the dispersion of copper, the BET surface area, and the surface area of copper and ZnO. The dispersion of copper was determined by the N_2O titration at 333 K (30). The surface area of ZnO was estimated by subtraction of that of copper from the BET surface area of the catalyst. For the estimation of the surface area of copper, the number of copper atoms exposed per square meter of copper was assumed to be 1.46×10^{19} atoms/m^2 (31) for the entire range of the catalyst composition.

Reaction

The CO_2–H_2 and CO–H_2 reactions were carried out in a flow reactor at atmospheric pressure (1 atm = 101.3 kPa). The gases in the inflow were purified by passage through a trap immersed in methanol containing dry ice. The gaseous composition in the outflow from the reactor was followed in time by gas chromatography. Helium was used as diluent.

Temperature Programmed Desorption

TPD runs were carried out over 1.0 g of the catalyst under a helium or a N_2 stream at a flow rate of 200 cm^3/min. After exposure to a stream of CO_2–H_2, CO–H_2, or H_2–He mixture at a flow rate of 200 cm^3/min, the catalyst was rapidly cooled to 353 K in the mixture. Gases in the reactor were flushed with a helium or N_2 stream and the catalyst was subsequently cooled to room temperature. The temperature was ramped at a rate of 5 K/min. The effluent from the reactor was analyzed by gas chromatography.

Diffuse Reflectance FT-IR Spectroscopy

FT-IR spectra of adsorbed species were recorded under He at room temperature with an infrared spectrophotometer (JASCO FT-IR-5M) to which a diffuse reflectance equipment (JASCO DR-500/H) was attached. The catalyst was placed in a cell and subjected to exposure to gaseous mixtures of various compositions at elevated temperatures. Unless noted, a spectrum of the catalyst, which was reduced at 523 K and then treated under flowing He at 583 K, was used as the background.

RESULTS AND DISCUSSION

Mechanism of the Methanol Synthesis from CO_2

Reaction. When a CO_2–H_2 mixture ($CO_2/H_2 = 1/9$) was fed over the Cu/ZnO catalysts, CH_3OH was produced together with CO and H_2O. The methanol synthesis, $CO_2 + 3H_2 \rightarrow CH_3OH + H_2O$, occurred along with the reverse water gas shift reaction, $CO_2 + H_2 \rightarrow CO + H_2O$. The outlet partial pressure of CH_3OH and CO varied with time differently. CO was rapidly formed and then decreased to a steady-state value within a few minutes. By contrast, methanol increased slowly in a monotonic manner. A steady-state value was obtained after 2–3 h. These findings suggested that CH_3OH and CO were produced through parallel pathways.

XPS and Auger spectra of the catalyst revealed that metallic copper and zinc oxide were present before and after the reaction (32). No other species, such as Cu(I) and Cu(II), were detected. This suggested that the variation of the outlet partial pressure of methanol under the transient state did not result from a creation of new surface sites such as monovalent copper. Hence, the length of the induction period was governed by the kinetics of the methanol formation.

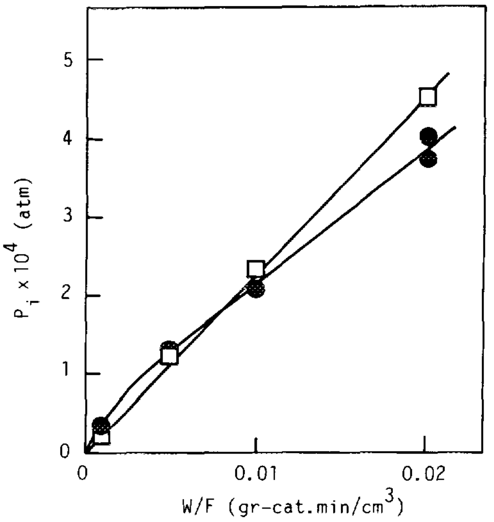

FIG. 1. Outlet partial pressure of CH_3OH (●) and CO (□) as a function of W/F. The CO_2–H_2 (CO_2/H_2 = 1/9) reaction was carried out over a 30 mol% Cu/ZnO catalyst at 438 K.

Figure 1 illustrates the variation of the outlet partial pressure of CH_3OH and CO at the steady state with *W/F* (*W*, weight of the catalyst used; *F*, total flow rate) of the reaction. The outlet partial pressures of both CH_3OH and CO increase with the increased *W/F*. Figure 2 plots the selectivities to methanol obtained at different temperatures against the conversion of CO_2. The selectivity to methanol increases with the decreased conversion of CO_2. It always approaches the *y*-axis at a value less than 100% at zero CO_2 conversion. The selectivity to methanol production increases with decreasing reaction temperature. These findings also suggest that the methanol synthesis and the reverse water gas shift reaction proceed through parallel pathways.

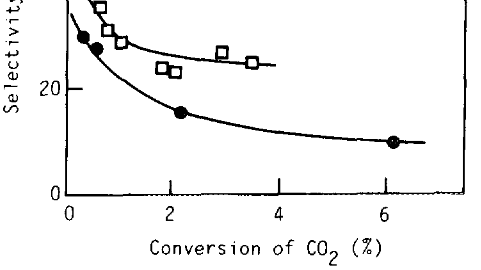

FIG. 2. Selectivity to methanol versus the conversion of CO_2. The CO_2–H_2 reaction was carried out over 30 mol% Cu/ZnO at 438 K (○), 463 K (□), and 483 K (●).

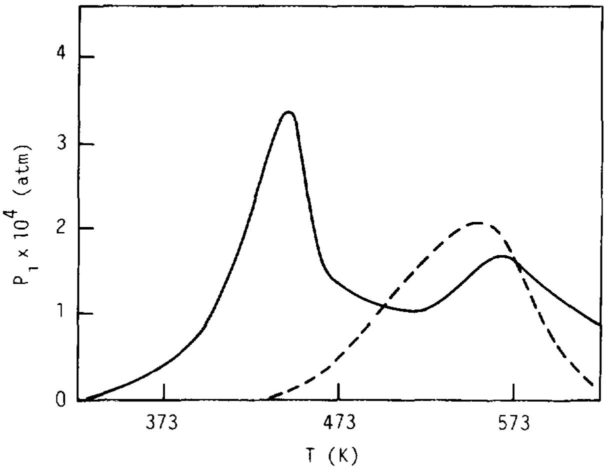

FIG. 3. TPD spectra of CO_2 (——) and CO (---) obtained after the CO_2–H_2 reaction was carried out at 438 K for 4 h over the 30 mol% Cu/ZnO catalyst.

Adsorbed species. Figure 3 illustrates the TPD profiles of CO_2 and CO obtained after the reaction attained a steady state over the 30 mol% Cu/ZnO. Two CO_2 peaks are observed at 443 K (α-CO_2) and at 563 K (β-CO_2), and one CO peak is observed at 553 K (α-CO). These peaks were always accompanied by H_2 peaks at the same temperatures. No H_2O desorbed in the course of the TPD run. For the catalyst treated with formic acid at room temperature, strong peaks ascribed to α- and β-CO_2 appeared with a weak one ascribed to α-CO. The intensity of the CO peak was practically negligible as compared with that of the CO_2 peaks. For the catalyst treated with CH_3OH, an intense CO peak was observed at 563 K, which could be ascribed to α-CO. These findings suggest that α- and β-CO_2 be ascribed to formate species, α-CO to methoxide species.

TPD profiles of CO_2 and CO obtained over the other Cu/ZnO catalysts (10, 50, 70, and 90 Cu–mol%) were similar to those illustrated in Fig. 3, while only one small peak of CO_2, assignable to α-CO_2, was observed at 440 K over the pure copper catalyst.

Figure 4 plots the amount of α-CO_2 estimated from the peak area in the TPD runs against that of the surface metallic copper atoms. The former value increases in proportion to the latter value, suggesting that the α-CO_2 peak arose from the surface species adsorbed on the copper sites.

Figure 5 shows the relationship between the amount of β-CO_2 and the surface area of ZnO present in the Cu/ZnO catalysts. The amount of β-CO_2 increases almost in proportional to the surface area of ZnO, although the

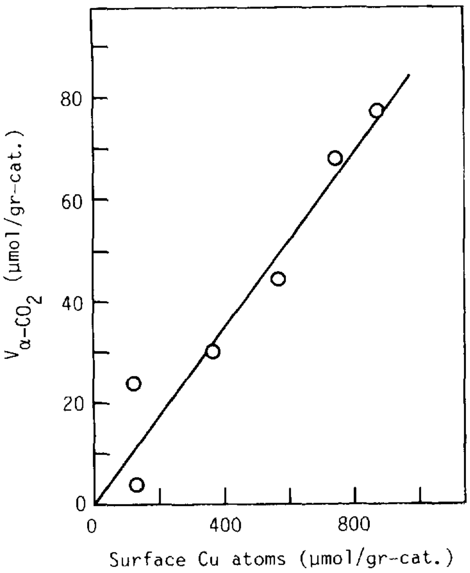

FIG. 4. Relationship between the amount of α-CO_2 and that of the surface metallic copper atoms.

curve is somewhat convex upward. This suggests that the β-CO_2 peak originated from the surface species adsorbed on ZnO.

In contrast, the amount of α-CO correlated with neither the surface area of copper nor ZnO.

An IR spectrum was measured for a 30 mol% Cu/ZnO catalyst previously subjected to the CO_2–H_2 reaction at 438 K (26). It showed that copper formate (HCOO–Cu: 2930, 2850, 1620, 1350 cm^{-1}), zinc formate (HCOO–Zn: 2970, 2880, 2740, 1580, 1383, 1365 cm^{-1}), and zinc methoxide (CH_3O–Zn: 2930, 2825, 1060 cm^{-1}) were formed in the course of the CO_2–H_2 reaction. After the catalyst was exposed to flowing He for 10 min at 438 K, where the desorption of α-CO_2 was completed, the IR absorption band for HCOO–Cu decreased appreciably. The intensities of other IR absorption bands remained unchanged at this temperature. They vanished at 573 K where the desorption of β-CO_2 and α-CO were completed.

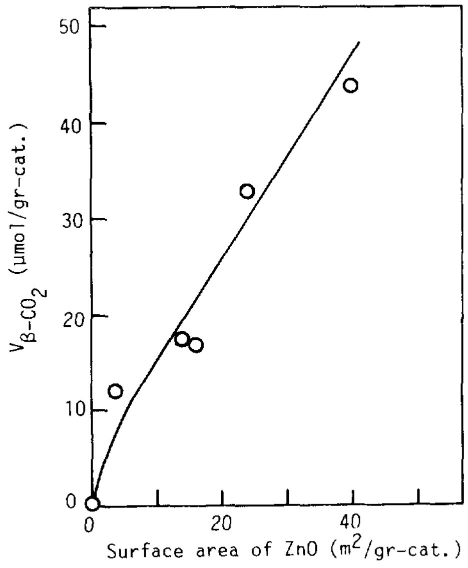

FIG. 5. Relationship between the amount of β-CO_2 and the surface area of ZnO upon Cu/ZnO.

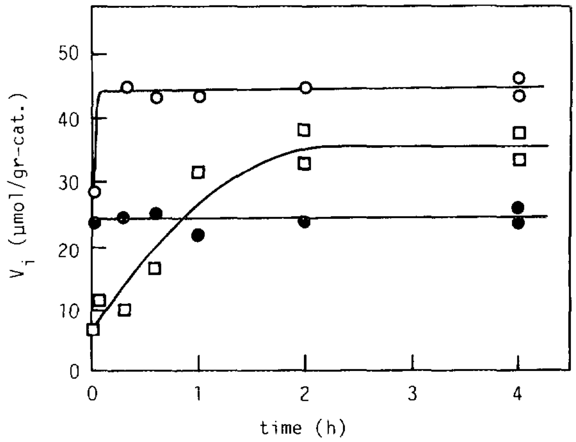

FIG. 6. Variation of the amounts of HCOO-Cu (○), HCOO-Zn (●), and CH_3O-Zn (□) with time in the course of the CO_2–H_2 reaction over 30 mol% Cu/ZnO.

Combining the results obtained by the TPD method and IR spectroscopy, we concluded that α-CO_2, β-CO_2, and α-CO peaks originated from HCOO–Cu, HCOO–Zn, and CH_3O–Zn, respectively.

Figure 6 shows how the amounts of HCOO–Cu, HCOO–Zn, and CH_3O–Zn vary with time in the CO_2–H_2 reaction over the 30 mol% Cu/ZnO catalyst. The amounts of HCOO–Cu and HCOO–Zn increase rapidly and reach steady-state values within a few minutes. By contrast, the amount of CH_3O–Zn increases slowly with time and attains a constant value after 2 h. In conformity with these observations, only the IR absorption bands for CH_3O–Zn increased in intensity with time and reached their steady-state values, while those for HCOO–Cu and HCOO–Zn were at constant intensities.

In a similar manner, experiments were also carried out at a different total flow rate. When the CO_2–H_2 reaction was carried out at a flow rate of 100 cm^3/min, the amounts of CH_3O–Zn produced during the initial 10 min and 1 h were 8 and 28 μmol/g-cat., respectively. A comparison of these values with the variation of the amount of CH_3O–Zn illustrated in Fig. 6, which was obtained at a flow rate of 200 cm^3/min, showed that the amount of CH_3O–Zn under the transient state was unaffected by the total flow rate. In contrast with this, the outlet partial pressure of methanol under the transient state increased nearly in inverse pro-

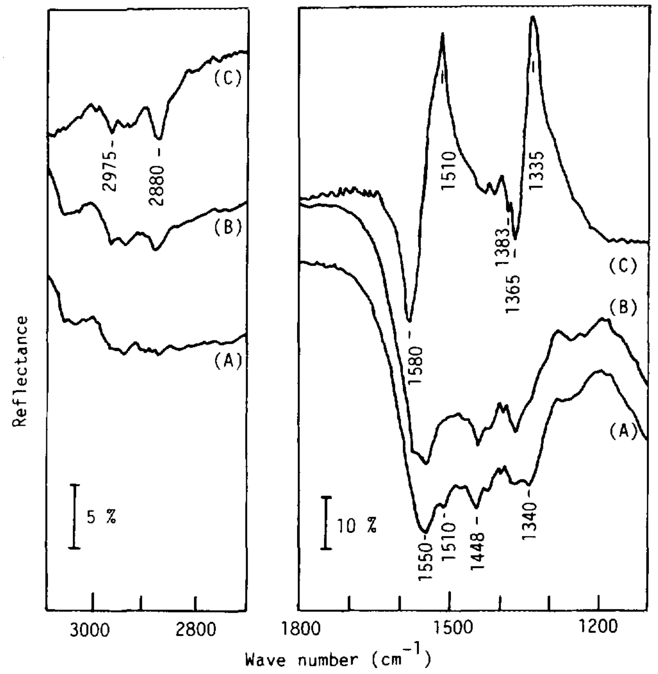

FIG. 7. Diffuse reflectance IR spectra of the catalyst. (A) After the helium treatment at 373 for 10 min following CO_2 adsorption at room temperature, (B) after H_2 was fed at 373 K for 60 min over the catalyst treated under the same conditions as A, and (C) a ratio spectrum of A/B. For the spectra A and B, a spectrum of KBr was used as the background.

portion to the total flow rate. These findings strongly suggested that the formation of CH_3O–Zn was unaffected by the presence of methanol under the present experimental conditions, and hence the readsorption of methanol from the gas phase was practically negligible for the formation of CH_3O–Zn.

In the following sections, the formation of the surface species was investigated in more detail by the TPD method and IR spectroscopy over the 30 mol% Cu/ZnO catalyst for the elucidation of the reaction mechanism of the methanol synthesis.

Formation of formate species. After CO_2 was adsorbed on the catalyst at room temperature, the catalyst was treated under a helium flow at 373 K for 10 min and subsequently spectrum A in Fig. 7 was recorded. Thereafter, the helium flow was switched to a flow of a H_2–He mixture (partial pressure of H_2 = 0.9 atm) for 60 min and spectrum B was obtained. On the switch to the mixture, IR absorption bands ascribable to HCOO–Zn appear at 2970 and 2880 cm^{-1}. Spectrum C shows the ratio spectrum of A/B. It is evident that the IR absorption bands for HCOO–Zn (2970, 2880, 1580, 1383, 1365 cm^{-1}) grow at the expense of the absorption bands at 1510 and 1335 cm^{-1}.

ZnO alone was subjected to the adsorption of CO_2 at room temperature and treated with flowing helium at elevated temperatures. It exhibited strong absorption bands at 1510 and 1335 cm^{-1} together with that at 1030 cm^{-1}. According to the results obtained on ZnO by Saussey *et al.* (33), these bands were assigned to polydentate carbonates. Hence, we concluded that HCOO–Zn was produced by the hydrogenation of the surface carbonate species formed on the ZnO support over Cu/ZnO.

Experiments were also carried out over ZnO having the surface carbonate. It was found that the surface carbonate species were hydrogenated to HCOO–Zn on ZnO alone. However, the observed rate of HCOO–Zn formation was much lower than that over the Cu/ZnO catalyst. The rate based on the ZnO surface area for the Cu/ZnO catalyst was estimated to be 30 times that for the ZnO alone. This strongly suggests that the HCOO–Zn formation was accelerated in the presence of Cu. Over Cu/ZnO, hydrogen adatoms formed at Cu sites probably spilled over to ZnO sites and reacted with the carbonate species.

The mechanism of the formation of HCOO–Cu was still ambiguous. When an IR spectrum was measured after CO_2 alone was adsorbed on Cu/Zn, absorption bands of CO_2 adsorbed on copper sites were indistinguishable due to the absorption bands of the surface species formed on the ZnO support. CO_2 species or carbonate species formed on copper sites may be responsible for the formation of HCOO–Cu, as other authors proposed (19, 34–36).

Formation of CH_3O–Zn. HCOO–Zn and HCOO–Cu were produced over the catalyst from a CO_2–H_2 mixture at 438 K, and subsequently the HCOO–Cu was removed by decomposition in flowing helium at 463 K. The hydrogenation of HCOO–Zn was then carried out for given periods of time in a stream of H_2 at various temperatures. Thereafter, the temperature was rapidly lowered to room temperature. Gases in the reactor were flushed with helium and the amounts of the surface species were determined by the TPD method.

When a stream of H_2 was fed over the catalyst having HCOO–Zn, the α-CO peak increased with time and the β-CO_2 peak decreased. This indicated that CH_3O–Zn grows at the expense of HCOO–Zn. Figure 8 illustrates the variation of the amounts of HCOO–Zn and CH_3O–Zn in the course of the hydrogenation at 438 K. The amount of CH_3O–Zn formed is practically the same as the amount of HCOO–Zn decreased. This led to the conclusion that CH_3O–Zn was produced via the hydrogenation of HCOO–Zn.

Similar experiments were also carried out at different partial pressure of H_2 or over the catalyst having different amounts of HCOO–Zn. The amount of CH_3O–Zn formed was followed in time by the TPD method. From the plot of the amount of CH_3O–Zn against time, the rate of the CH_3O–Zn formation was evaluated. In Figs. 9 and 10, the initial turnover frequencies were plotted against the partial

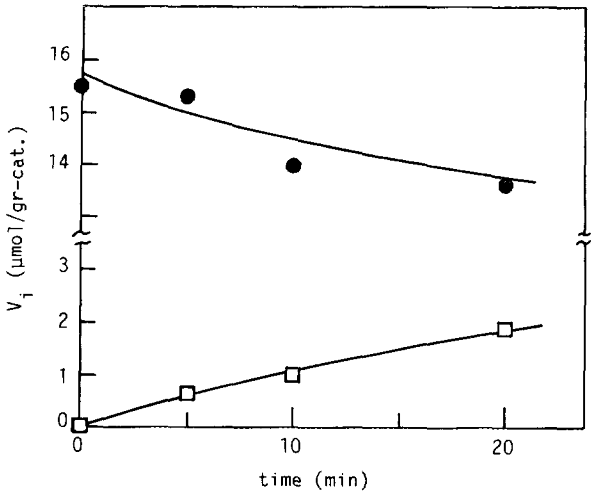

FIG. 8. Variation of the amounts of HCOO–Zn (●) and CH_3O–Zn (□) in the course of the hydrogenation of HCOO–Zn at 438 K. Partial pressure of H_2 was 0.9 atm.

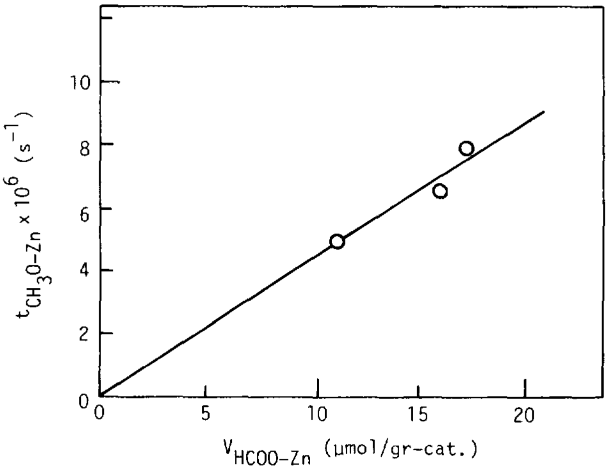

FIG. 10. The initial turnover frequency of CH_3O–Zn versus the amount of HCOO–Zn preadsorbed on the catalyst.

pressure of H_2 and the amount of HCOO–Zn preadsorbed, respectively. It is shown that the turnover frequency is proportional to both of the partial pressure of H_2 and the amount of HCOO–Zn species.

Experiments were also carried out for HCOO–Zn formed on ZnO alone. No CH_3O–Zn was produced by the reaction between HCOO–Zn and H_2. This suggests that the hydrogenation of HCOO–Zn was markedly enhanced over Cu/ZnO. Hence, it was again suggested that hydrogen activated at Cu sites was responsible for the hydrogenation of HCOO–Zn over Cu/ZnO.

The hydrogenation of HCOO–Cu species was also conducted at temperatures below 400 K, where HCOO–Cu was thermally stable. After HCOO–Cu and HCOO–Zn species were prepared from the mixture of CO_2 and H_2, gases in the reactor were flushed with flowing He at 353 K. The temperature was then raised rapidly to 383 K and the hydrogenation of HCOO–Cu was conducted for various periods of time. Variations of the amounts of the surface species in the hydrogenation were also followed by the TPD method. Figure 11 illustrates how the amounts of HCOO–Cu, HCOO–Zn, and CH_3O–Zn species vary in the course of the hydrogenation at 383 K. The amount of HCOO–Zn remains unchanged during the course of the experiment, whereas that of HCOO–Cu decreases and that of CH_3O–Zn increases with time. Hence, CH_3O–Zn was produced through the hydrogenation of HCOO–Cu in

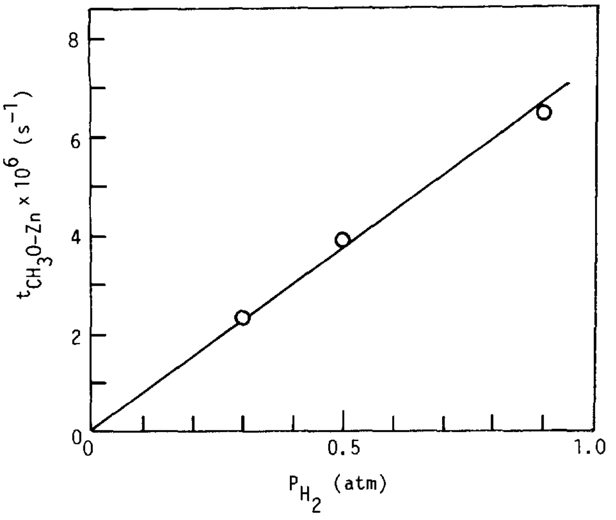

FIG. 9. The initial turnover frequency of CH_3O–Zn formation versus the partial pressure of H_2.

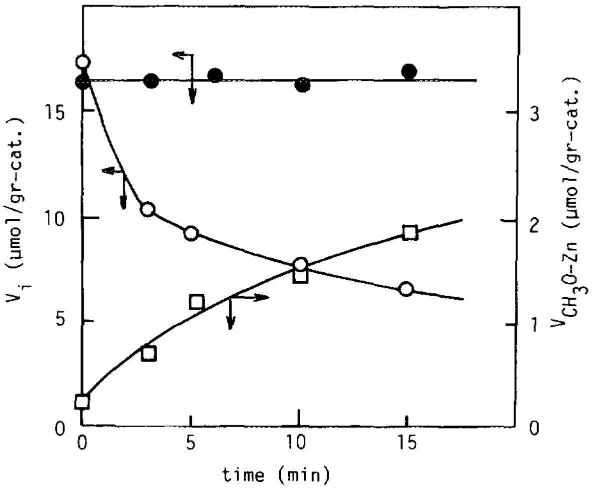

FIG. 11. Variation of the amounts of HCOO–Cu (○), HCOO–Zn (●), and CH_3O–Zn (□) with time in the course of the H_2 treatment at 383 K over the catalyst preadsorbed with HCOO–Cu and HCOO–Zn.

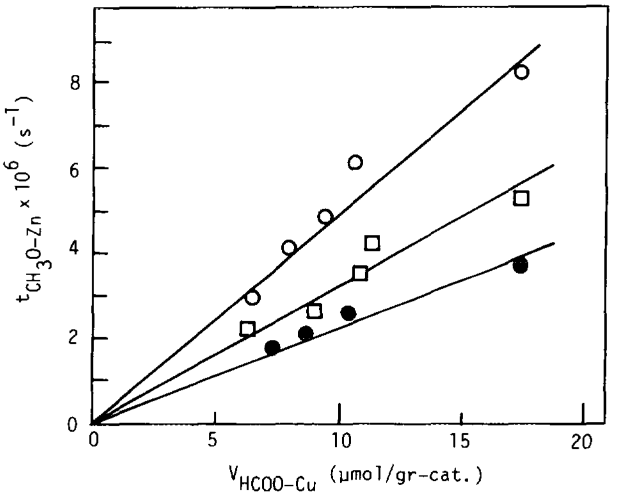

FIG. 12. Relationship between the turnover frequency of CH_3O–Zn formation and the amount of HCOO–Cu at various partial pressures of H_2. P_{H_2} = 0.9 atm (○), 0.5 atm (□), and 0.3 atm (●).

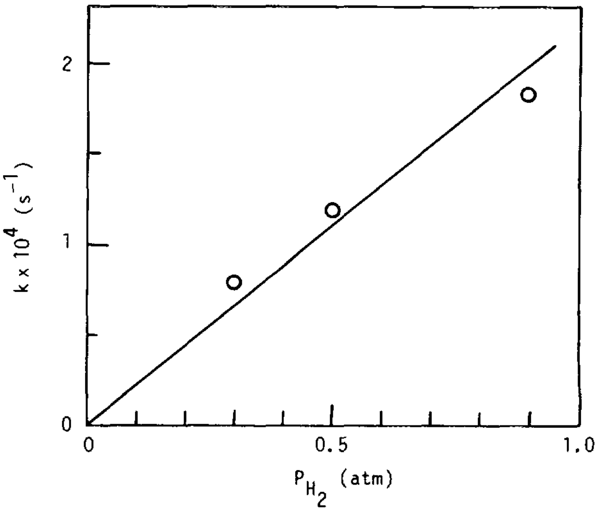

FIG. 13. Relationship between the rate constant of the CH_3O–Zn formation from HCOO–Cu and the partial pressure of H_2.

preference to the hydrogenation of HCOO–Zn. However, the amount of HCOO–Cu decreased was not equivalent to that of CH_3O–Zn formed. This was probably caused by the slow decomposition of HCOO–Cu to CO_2 and H_2.

The turnover frequency of CH_3O–Zn formation was estimated from the slope of the curve shown in Fig. 11. Figure 12 shows the turnover frequencies obtained at various partial pressures of H_2 against the amount of HCOO–Cu. It demonstrates that the rate of the CH_3O–Zn formation is proportional to the amount of HCOO–Cu.

The rate constant of the CH_3O–Zn formation from HCOO–Cu was estimated from the slope of the line in Fig. 12, and is plotted against the partial pressure of H_2 in Fig. 13. This shows that the rate of CH_3O–Zn formation from HCOO–Cu is proportional to the partial pressure of H_2.

The hydrogenation reactions of HCOO–Zn and HCOO–Cu were also carried out at various temperatures. Figure 14 plots the rate constants obtained for these reactions against the reciprocal of the temperature. Under the present reaction conditions, the rate constant of the hydrogenation of HCOO–Cu is about 10 times greater than that of the hydrogenation of HCOO–Zn. The activation energies are determined at 61.4 and 51.6 kJ/mol, respectively, for the hydrogenation of HCOO–Zn and the hydrogenation of HCOO–Cu. Thus, the turnover frequencies of the hydrogenation of HCOO–Zn to CH_3O–Zn ($t'_{CH_3O\text{-}Zn}$) and of the HCOO–Cu to CH_3O–Zn ($t_{CH_3O\text{-}Zn}$) can be expressed, respectively, as

$$t'_{CH_3O\text{-}Zn} = 9.18 \times 10^6 \exp(-61400/RT) V_{HCOO\text{-}Zn} P_{H_2} \quad [1]$$

and

$$t_{CH_3O\text{-}Zn} = 5.69 \times 10^6 \exp(-51600/RT) V_{HCOO\text{-}Cu} P_{H_2}, \quad [2]$$

where $V_{HCOO\text{-}Zn}$ and $V_{HCOO\text{-}Cu}$ represent the amount of HCOO–Cu and HCOO–Cu, respectively, in units of mol/g-cat. Turnover frequencies are in units of s^{-1}, and P_{H_2}, the partial pressure of H_2, is in units of atm.

Formation of methanol from CH_3O–Zn. It was previously shown that CH_3O–Zn was rapidly hydrolyzed to methanol in the course of the methanol synthesis from CO_2 (26). When a mixture of CO_2–H_2 was fed over the

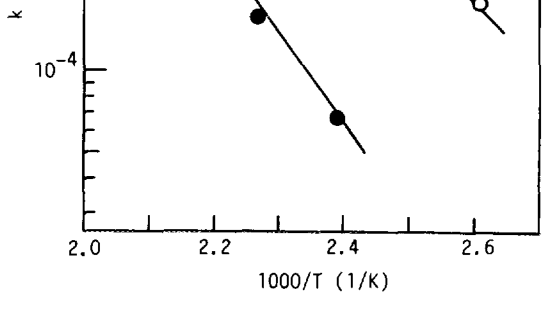

FIG. 14. Rate constants of the hydrogenation of HCOO–Cu (○) and HCOO–Zn (●) versus the reciprocal of the temperature.

catalyst on which various amounts of CH_3O–Zn were previously produced by the reaction with CO_2–H_2 at 438 K or methanol adsorption at room temperature followed by a He treatment at 438 K, the outlet partial pressure of methanol in the effluent was rapidly increased and reached a steady state value. The steady state of the methanol formation was attained more rapidly with the increased amount of CH_3O–Zn previously adsorbed. When the amount of the preadsorbed CH_3O–Zn was in excess of that at the steady state, the outlet partial pressure of methanol overshot the steady-state value. In contrast, when H_2 or CO_2 alone was fed over the catalyst having CH_3O–Zn, no methanol was produced. However, on feeding of H_2O, methanol was detected in the effluent even at a lower temperature, 383 K. These findings strongly suggested that methanol was produced via hydrolysis of CH_3O–Zn. Consistent with this, the IR absorption bands of CH_3O–Zn decreased on feeding of H_2O. On the basis of these findings, we concluded that CH_3O–Zn was effectively hydrolyzed by H_2O formed via the reverse water shift reaction, being transformed to methanol in the course of the methanol synthesis.

Mechanism of the methanol synthesis from CO_2. As shown above, the hydrolysis of CH_3O–Zn, as well as the formation of HCOO–Zn and HCOO–Cu, was facile. Hence, one of the steps involved in the hydrogenation of HCOO–Zn and HCOO–Cu to CH_3O–Zn would be the rate determining step in the methanol synthesis from CO_2. For discussion on the involvement of HCOO–Zn and HCOO–Cu in the methanol synthesis, the rates of the hydrogenation of HCOO–Zn and HCOO–Cu were compared with that of the methanol synthesis at the temperature of 438 K. By analysis with FT-IR spectroscopy and the TPD method, the amounts of HCOO–Zn and HCOO–Cu at the steady state of the reaction were estimated to be 24.6 and 44.3 μmol/g-cat., respectively, at the respective partial pressures of CO_2 and H_2 of 0.1 and 0.9 atm. By use of these values, the turnover frequencies of the CH_3O–Zn formation from HCOO–Zn and HCOO–Cu were evaluated to be 1.07×10^{-5} and 1.59×10^{-4} s^{-1} at a hydrogen partial pressure of 0.9 atm, respectively, from Eqs. [1] and [2].

On the other hand, the observed turnover frequency of the methanol synthesis was estimated to be 7.35×10^{-5} s^{-1} at a W/F value for 0.001 g-cat. min/cm^3 from Fig. 1. The observed rate was close to that of the hydrogenation of HCOO–Cu, although the former rate was lower than the latter rate by a factor of 2 times.

A slower rate of methanol synthesis than that of the hydrogenation of HCOO–Cu would be ascribed to H_2O being produced and/or to the presence of CO_2 in the former reaction. Bardet *et al.* (37) previously showed that the methanol synthesis from CO_2 over $Cu/ZnO/Al_2O_3$ was suppressed by H_2O. As Fig. 1 showed, the curve of methanol is slightly convex upward, suggesting that a small amount of H_2O retarded the methanol synthesis. Furthermore, Fu and Somorjai (38) suggested that H_2 and CO_2 adsorbed the same sites on the Cu(311) single crystal. If CO_2 competitively adsorbed on the same sites as H_2 on Cu/ZnO, the sites available for H_2 adsorption should decrease in the presence of CO_2. Hence, the hydrogenation of HCOO–Cu would decrease in the methanol synthesis from CO_2 because of the presence of CO_2 in the gas phase.

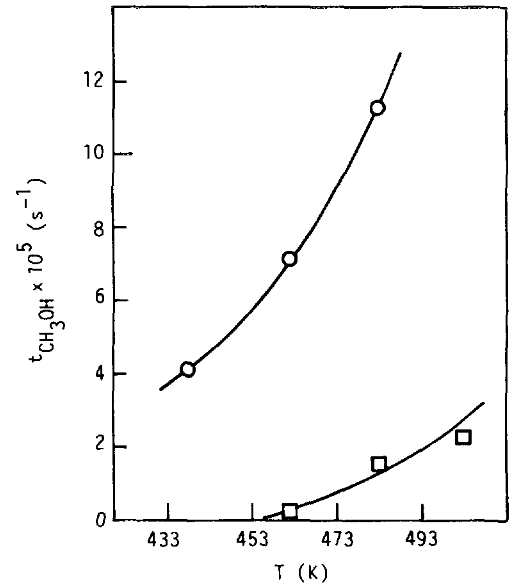

FIG. 15. Comparison of the turnover frequency of the methanol synthesis from CO_2 (○) and that from CO (□) over the 30 mol% Cu/ZnO catalyst. P_{CO_2}, P_{CO} = 0.1 atm, P_{H_2} = 0.9 atm.

Based on these findings, we concluded that the methanol synthesis from CO_2 proceeded as

$$\begin{tikzcd} & & HCOO\text{-}Zn & & \\ CO_2 \arrow[r, "{Cu, ZnO}"'] & CO_2(a) \text{ or } CO_3(a) \arrow[ur, "H_2"] \arrow[r, "H_2"'] & HCOO\text{-}Cu \arrow[r, "H_2"'] & CH_3O\text{-}Zn \arrow[r, "H_2O"'] & CH_3OH, \end{tikzcd}$$

in which HCOO–Cu was involved.

Mechanism of the Methanol Synthesis from CO

Figure 15 compares the rate of the methanol synthesis from CO_2 with that from CO over the 30 mol% Cu/ZnO catalyst. It is clear that methanol is produced more rapidly from CO_2 than from CO. No methanol is produced from CO below 438 K, at which the mechanism of methanol synthesis from CO_2 was studied in the preceding sections.

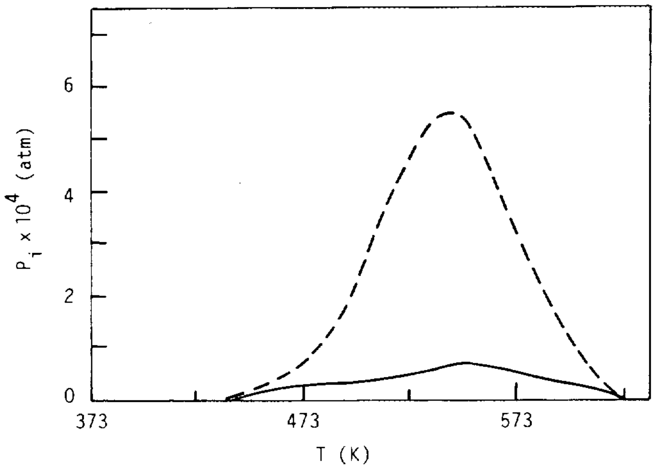

FIG. 16. TPD spectra of CO_2 (——) and CO (---) obtained after the CO–H_2 mixture was fed over the catalyst at 438 K for 4 h.

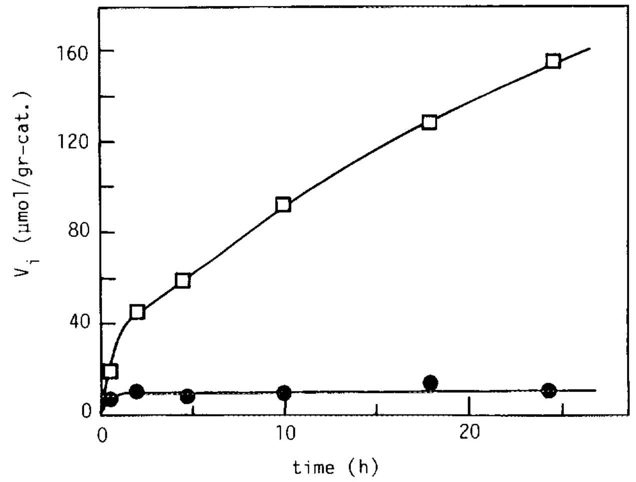

FIG. 17. Variation of the amounts of HCOO–Zn (●) and CH_3O–Zn (□) with time in the course of feeding the CO–H_2 mixture.

Figure 16 illustrates TPD spectra of CO and CO_2 obtained after a CO–H_2 mixture (CO/H_2 = 1/9) was fed over the Cu/ZnO catalyst at 438 K for 4 h. A strong peak of α-CO is observed together with a weak peak of β-CO_2. No β-CO_2 peak appears. Consistent with these findings, strong absorption bands for CH_3O–Zn were observed along with those of HCOO–Zn in the IR spectra of the catalyst treated with the mixture of CO–H_2. No absorption bands ascribed to HCOO–Cu occurred.

It has been shown that HCOO–Zn was produced via the reaction of CO with surface hydroxyl species over ZnO (39, 40). A similar process was probably involved in the synthesis of methanol from CO over the Cu/ZnO catalyst as observed by Edwards and Schrader (17).

The CO–H_2 reaction was carried out for various periods of time and then the amounts of CH_3O–Zn and HCOO–Zn produced in the course of the reaction were determined by the TPD method. Figure 17 illustrates the variation of the amounts of these species in the course of the reaction at 438 K. The amount of HCOO–Zn reaches the steady-state value instantly. The amount of CH_3O–Zn increases steadily with time for a period of over 24 h. It is to be noted that the amount of CH_3O–Zn formed in the first 24 h greatly exceeds that formed in the CO_2–H_2 reaction. It reaches a value five times greater than that in the latter reaction. As opposed to these observations, no methanol was produced in the gas phase.

The turnover frequency of the CH_3O–Zn formation was estimated from the slope of the line in Fig. 17 in which the amount of CH_3O–Zn increased linearly with time. The turnover frequency thus estimated was $4.6 \times 10^{-6}\ s^{-1}$. On the other hand, by making use of Eq. [1] and the amount of HCOO–Zn (10 μmol/g-cat., see Fig. 17) present in the CO–H_2 reaction, we evaluated the turnover frequency of CH_3O–Zn formation to be $4.5 \times 10^{-6}\ s^{-1}$. This coincided well with the turnover frequency obtained from the plot in Fig. 17. Hence, we concluded that CH_3O–Zn was formed via the hydrogenation of HCOO–Zn in the course of the CO–H_2 reaction.

When H_2O was fed over the catalyst having CH_3O–Zn prepared from the CO–H_2 mixture, the amount of CH_3O–Zn decreased rapidly and methanol was detected in the effluent even at 383 K, as observed in the system of CO_2–H_2.

When a CO–H_2 mixture was switched to the CO–H_2 mixture containing a small amount of H_2O, methanol was produced even at 438 K. Figure 18 illustrates how the outlet partial pressure of methanol varies with time upon switching to the CO–H_2–H_2O mixture. In the absence of H_2O,

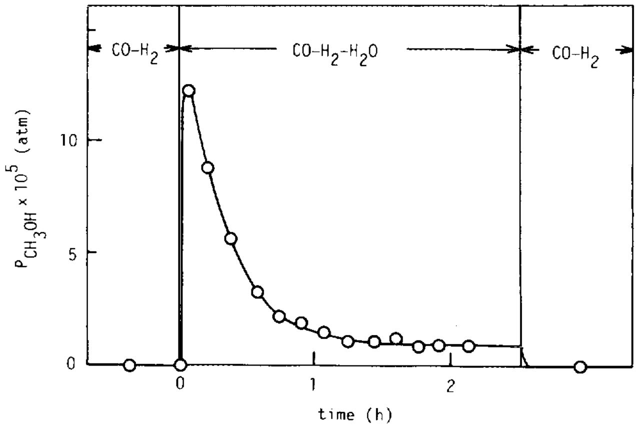

FIG. 18. Variation of the outlet partial pressure of methanol with time. A CO–H_2 mixture was switched to CO–H_2–H_2O and then the mixture was switched again to CO–H_2. The temperature was 438 K. Partial pressures of CO, H_2, and H_2O were 0.1, 0.7, and 4×10^{-4} atm, respectively.

no methanol is detected in the effluent. After the switch to the CO–H_2–H_2O mixture, the methanol formation increases rapidly and then decreases to a steady-state value. When the mixture was again switched to the CO–H_2 mixture, the methanol formation ceased. These findings indicate that the conversion of CH_3O–Zn to methanol was markedly lowered in the CO–H_2 reaction because of the absence of H_2O in the gas phase. Hence, a great amount of CH_3O–Zn accumulated in the course of the CO–H_2 reaction, as seen in Fig. 17.

In contrast to the observations at 438 K, methanol is slowly formed in the CO–H_2 reaction above 460 K, as Fig. 15 shows. Under these conditions, CH_3O–Zn would slowly react with surface hydroxyl species over ZnO, being transformed to methanol.

Hence, we concluded that methanol synthesis from CO over the Cu/ZnO catalyst proceeded as

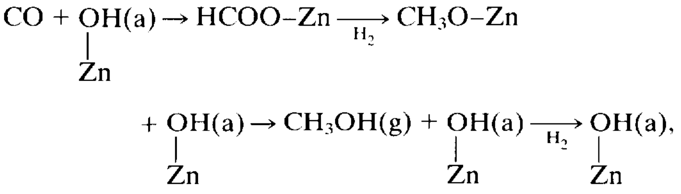

$$\mathrm{CO} + \underset{\displaystyle\mathrm{Zn}}{\underset{|}{\mathrm{OH(a)}}} \rightarrow \mathrm{HCOO{-}Zn} \xrightarrow[\mathrm{H_2}]{} \mathrm{CH_3O{-}Zn}$$

$$+ \underset{\displaystyle\mathrm{Zn}}{\underset{|}{\mathrm{OH(a)}}} \rightarrow \mathrm{CH_3OH(g)} + \underset{\displaystyle\mathrm{Zn}}{\underset{|}{\mathrm{OH(a)}}} \xrightarrow[\mathrm{H_2}]{} \underset{\displaystyle\mathrm{Zn}}{\underset{|}{\mathrm{OH(a)}}},$$

in which HCOO–Zn and surface hydroxyl were involved.

Difference in the Rate between the Methanol Synthesis from CO_2 and from CO

In the preceding sections, we showed that methanol synthesis from CO_2 occurred rapidly as compared to that from CO. The former reaction proceeded through the hydrogenation of HCOO–Cu to CH_3O–Zn, whereas the latter reaction proceeded through the hydrogenation of HCOO–Zn to CH_3O–Zn. HCOO–Cu was absent in the CO–H_2 reaction. Under the present reaction conditions, the rate of the hydrogenation of HCOO–Cu was faster than that of the hydrogenation of HCOO–Zn by a factor of 10 (Fig. 14). The rate of the transformation of CH_3O–Zn to methanol in the CO_2–H_2 reaction was much faster than that in the CO–H_2 reaction. Therefore, the difference in rates between methanol synthesis from CO_2 and from CO was ascribed to the difference in the reactivity of HCOO–Cu and HCOO–Zn involved in the formation of CH_3O–Zn and the presence or the absence of H_2O in the conversion of CH_3O–Zn to methanol. At lower temperatures, the presence of H_2O may cause the great difference between the rates of the methanol synthesis from CO_2 and from CO. Under such conditions, the methanol formation from CH_3O–Zn was markedly enhanced in the CO_2–H_2 reaction because of the formation of H_2O via the reverse water gas shift reaction occurring with the methanol synthesis from CO_2.

REFERENCES

1. Denny, P. J., and Whan, D. A., *in* "Catalysis," Vol. 2, p. 46. Chem. Soc. London, 1978.
2. Klier, K., *in* "Advances in Catalysis" (D. D. Eley, H. Pines, and P. B. Wisz, Eds.), Vol. 31, p. 243. Academic Press, New York, 1982.
3. Bart, J. C. J., and Sneeden, R. P. A., *Catal. Today* **2,** 1 (1987).
4. Chinchen, G. C., Denny, P. J., Jennings, J. R., Spencer, M. S., and Waugh, K. C., *Appl. Catal.* **36,** 1 (1988).
5. Rozovskii, A. Y., *Kinet. Katal.* **21,** 97 (1980).
6. Bardet, R., Thivoll-Cazat, J., and Trambouze, Y., *J. Chim. Phys. Phys. Chim. Biol.* **78,** 135 (1981).
7. Denise, B., and Sneeden, R. P. A., *J. Mol. Catal.* **17,** 359 (1982).
8. Ramarson, E., Kieffer R., and Kinnemann, A., *Appl. Catal.* **4,** 281 (1982).
9. Kuznetsov, V. D., Shub, F. S., and Temkin, M. I., *Kinet. Katal.* **23,** 932 (1982).
10. Amenomiya, Y., and Tagawa, T., *in* "Proceedings, 8th International Congress on Catalysis, Berlin, 1984." Vol. 2, p. 557. Dechema, Frankfurt-am-Main, 1984.
11. Baussart, H., Delobel, R., Le Bras, M., Le Maguer, D., and Leroy, J. M., *Appl. Catal.* **14,** 381 (1985).
12. Tagawa, T., Pleizier, G., and Amenomiya, Y., *Appl. Catal.* **18,** 285 (1985).
13. Bardet, R., Thivolle-Cazat, J., and Tranbouze, Y., *C_1 Mol. Chem.* **1,** 201 (1985).
14. Denise, B., and Sneeden, R. P. A., *Appl. Catal.* **28,** 235 (1986).
15. Amenomiya, Y., *Appl. Catal.* **30,** 57 (1987).
16. Denise, B., Cherifi, O., Bettahar, M. M., and Sneeden, R. P. A., *Appl. Catal.* **48,** 365 (1989).
17. Edwards, J. F., and Schrader, G. L., *J. Phys. Chem.* **88,** 5620 (1984).
18. Bowker, M., Hadden, R. A., Houghton, H., Hyland, J. N. K., and Waugh, K. C., *J. Catal.* **109,** 263 (1988).
19. Saussey, J., and Lavalley, J. C., *J. Mol. Catal.* **50,** 343 (1989).
20. Chauvin, C., Saussey, J., Lavalley, J. C., Idriss, H., Hindermann, J. P., Kiennemann, A., Chaumette, P., and Courty, P., *J. Catal.* **121,** 56 (1990).
21. Kiennemann, A., Idriss, H., Hindermann, J. P., Lavalley, J. C., Vallet, A., Chaumette, P., and Courty, P., *Appl. Catal.* **59,** 165 (1990).
22. Millar, G. J., Rochester, C. H., Bailey, S., and Waugh, K. C., *J. Chem. Soc. Faraday Trans.* **88,** 2085 (1992).
23. Robinson, W. R. A. M., and Mol., J. C., *Appl. Catal. A* **98,** 81 (1993).
24. Bussche, K. M. V., and Froment, G. F., *Appl. Catal. A* **112,** 37 (1994).
25. Idriss, H., Hindermann, J. P., Kieffer, R., Kiennemann, A., Vallet, A., Chauvin, C., Lavalley, J. C., and Chaumette, P., *J. Mol. Catal.* **42,** 205 (1987).
26. Fujita, S., Usui, M., Ohara, E., and Takezawa, N., *Catal. Lett.* **13,** 349 (1992).
27. Fujita, S., Ito, H., and Takezawa, N., *Bull. Chem. Soc. Jpn.* **66,** 3094 (1993).
28. Herman, R. G., Klier, K., Simmons, G. W., Finn, B. P., Bulko, J. B., and Kobylinski, T. P., *J. Catal.* **56,** 407 (1979).
29. Porta, P., Fierro, G., Lo Jacono, M., and Moretti, G., *J. Catal.* **109,** 367 (1988).
30. Sengupta, G., Gupta, D. K., Kundu, M. L., and Sen, S. P., *J. Catal.* **67,** 223 (1981).
31. Evans, J. W., Wainwright, M. S., Bridgewater, A., and Young, D. J., *Appl. Catal.* **7,** 75 (1983).

32. Fujita, S., Usui, M., and Takezawa, N., *J. Catal.* **134,** 220 (1992).
33. Saussey, J., Lavalley, J. C., and Bovet, C., *J. Chem. Soc. Faraday Trans.* **78,** 1457 (1982).
34. Burch, R., Chalker, S., and Pritchard, J., *J. Chem. Soc. Faraday Trans.* **87,** 193 (1991).
35. Millar, G. J., Rochester, C. H., and Waugh, K. C., *Catal. Lett.* **14,** 289 (1992).
36. Waugh, K. C., *Catal. Today* **15,** 51 (1992).
37. Bardet, R., Thivoll-Cazat, J., and Trambouze, Y., *C. R. Acad. Sci. Ser. 2* **299,** 423 (1984).
38. Fu, S. S., and Somorjai, G. A., *Surf. Sci.* **262,** 68 (1992).
39. Hussain, G., and Sheppard, N., *Spectrochim. Acta Part A* **43,** 1631 (1987).
40. Shido, T., and Iwasawa, Y., *J. Catal.* **129,** 343 (1991).